JOURNAL OF SOLID STATE CHEMISTRY 135, 17–27 (1998)
ARTICLE NO. SC977564

Superconducting $Sr_{2-x}A_xCuO_2F_{2+\delta}$ (A = Ca, Ba): Synthetic Pathways and Associated Structural Rearrangements

M. G. Francesconi,* P. R. Slater,*,[1] J. P. Hodges,* C. Greaves,*,[2] P. P. Edwards,* M. Al-Mamouri,* and M. Slaski†

*School of Chemistry, The University of Birmingham, Edgbaston, Birmingham, B15 2TT, United Kingdom; and †School of Physics and Space Research, The University of Birmingham, Edgbaston, Birmingham, B15 2TT, United Kingdom

Received March 4, 1997; in revised form July 16, 1997; accepted July 17, 1997

The low-temperature fluorination of a range of insulating alkaline earth cuprates $Sr_{2-x}A_xCuO_3$ (A = Ca ($0 \le x \le 2$); A = Ba ($0 \le x \le 0.6$)) can result in superconducting oxide fluorides $Sr_{2-x}A_xCuO_2F_{2+\delta}$. In contrast, conventional high-temperature solid–state reactions produce thermodynamically more stable mixtures of oxides and fluorides. Various soft-chemistry fluorination pathways (utilizing F_2 gas, NH_4F, MF_2 [M = Cu, Zn, Ni, Ag]) are compared with respect to their efficacy and mechanisms. Attention is also focused on the structural features of the mixed-oxide precursor and the final-oxide fluorides to highlight the remarkable structural rearrangements that occur during the low-temperature fluorination. The effects of fluorination of other Sr–Cu–O systems are used to identify the structural requirements of the precursor oxide in order to achieve such transformations.

INTRODUCTION

The discovery of high-temperature superconductivity in mixed-metal copper oxide systems initiated an unprecedented search for new and chemically modified superconductors. Although the vast majority of studies have focused on the wide range of *cation* substitutions which can be used to influence the structural and electronic characteristics of these compounds, chemical manipulation of the *anion* sublattices has more recently been shown to be an alternative in the search for new superconductors (1). In this context, studies of synthetic, structural, and electronic aspects of F^- for O^{2-} substitutions have been particularly important. In general, oxide structures are quite amenable to this substitution since the O^{2-} and F^- anions have similar radii (1.4 and 1.32 Å, respectively in sixfold coordination (2)). However, physical properties may differ markedly from those of the parent oxides and fluorides, since the anionic charge difference requires appropriate electronic compensation and, in addition, O^{2-} and F^- order can occur to produce superstructures. Although anisotropy can favor such ordering (3), in most phases the anions are in fact disordered. The structure of the parent oxide appears to determine the influence and extent of fluorine substitution—i.e., whether the structure is retained or significantly modified (e.g., by a rearrangement of the anion sublattice), and the degree to which physical properties are affected by the different charge and electronegativity of F^- compared to O^{2-}. Fluorination of oxides to form oxide fluorides can occur via (i) the substitution of one fluorine for one oxygen, (ii) the incorporation of two fluorines for each oxygen lost, or (iii) the insertion of fluorine into interstitial sites. All three possibilities are associated with either substantial structural, (ii), or electronic, (i) and (iii), changes. The latter normally result in either oxidation, (iii), or reduction, (i), of a transition metal ion during the fluorination process.

In the field of superconductivity research, fluorination studies have been reported on many compounds (see, for example, (4)), such as $REBa_2Cu_3O_{7-\delta}$ (RE = Y, lanthanide), materials with the simple structure types designated as T (La_2CuO_4), T^* ($La_{2-x}Nd_xSr_{0.15}CuO_4$; $0 \le x \le 1$) and T' (Nd_2CuO_4), and also on a range of bismuth and thallium containing compounds. The results have highlighted the potential of fluorine for the chemical control of electronic properties in order to induce or optimize superconductivity. Of particular importance are syntheses resulting in either simple substitution of F^- for O^{2-} (providing increased electron density in the superconducting "CuO_2" sheets) or insertion of F^0 into interstitial sites to yield F^- and provide a corresponding reduction in electron density.

Under mild conditions (typically using 10% F_2 in N_2 at 210°C), the reaction of F_2 gas wth Sr_2CuO_3 involves both substitution and insertion of fluorine to give the new superconducting oxide fluoride $Sr_2CuO_2F_{2+\delta}$ (5). Sr_2CuO_3 has a structure which is related to that of La_2CuO_4, but

[1] Present address: School of Chemistry, University of St. Andrews, St. Andrews, Fife, UK.

[2] To whom correspondence should be addressed.

0022-4596/98 $25.00

channels of oxygen vacancies disrupt the sheets of CuO_6 octahedra and linear chains of CuO_4 units are formed (Fig. 1). $Sr_2CuO_2F_{2+\delta}$ is even more closely related to La_2CuO_4, with layers of octahedrally coordinated Cu (5). Experimental evidence (5) showed that the substituting F^- ions avoid the equatorial positions, where the oxygen vacancies are located in the Sr_2CuO_3 structure, and reside only in apical sites. This observation has been supported by simple Madelung energy (5) and atomistic (6, 7) calculations. The insertion of fluorine into the channels therefore induces a structural rearrangement of the anion sublattice: the apical oxide ions migrate to equatorial sites in the Cu plane and are replaced by fluoride ions (Fig. 2). In this way, CuO_2 layers, which are thought essential for superconductivity, are formed and are separated by blocks of stoichiometry Sr_2F_2. The excess δF^- ions are located in interstitial sites—similar to those found in the superoxygenated and fluorinated materials $La_2CuO_{4+\delta}$ (8, 9) and $La_2CuO_4F_\delta$ (10)—to provide a composition $Sr_2CuO_2F_{2+\delta}$ (Fig. 3). The interstitial fluoride ions, F′ in Fig. 3, are responsible for the hole doping which ultimately makes this compound superconducting. Superconductivity with T_c up to 46 K is induced in this phase by mild postsynthesis reduction, and the maximum T_c occurs for a Cu oxidation state of approximately 2.3, corresponding to $\delta \approx 0.3$ (5). Theoretical calculations by Novikov *et al.* (11) support the view that optimum hole doping is expected at $\delta \approx 0.3$, and hence "as synthesized" samples with $\delta \approx 0.6$ are overdoped.

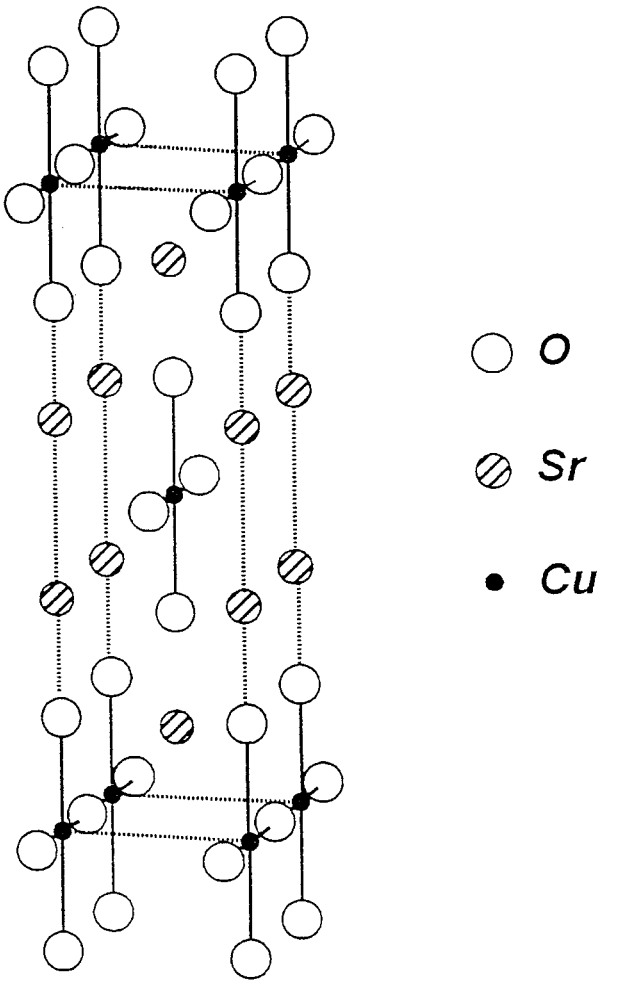

FIG. 1. Crystal structure of $(Sr/Ca)_2CuO_3$.

$Sr_2CuO_2F_{2+\delta}$ was the first example of a superconducting oxide fluoride in which F^- ions play a major structural role. In contrast to the fluorination of La_2CuO_4 to form $La_2CuO_4F_\delta$ (10), where oxidation occurs via incorporation of F^- ions into interstitial positions of a well-defined structure, in $Sr_2CuO_2F_{2+\delta}$ F^- ions not only provide similar electronic control but are also instrumental in the structural transformation of the "precursor" Sr_2CuO_3 into the new superconducting compound (5). We have also examined the structural and electronic effects of substituting Ca and Ba for Sr in $Sr_2CuO_2F_{2+\delta}$ to produce $Sr_{2-x}A_xCuO_2F_{2+\delta}$ (A = Ca, Ba), and T_c is increased by Ba substitution, with $T_c^{max} = 64$ K for $x = 0.6$ (12).

Following this initial demonstration of the potential of fluorine for forming new superconducting phases, subsequent work has led to the synthesis of other related superconducting oxide fluorides. For example, by means of high pressure, Kawashima *et al.* synthesized higher members in the same structural family ($Sr_2Ca_{n-1}Cu_nO_{2n+\delta}F_{2\pm y}$ with $n = 2$ and $n = 3$) which show critical temperature of 99 and 111 K, respectively (13).

Novikov *et al.* (11) and Kurmaev *et al.* (14) have examined the consequence of the lack of apical oxygen on the electronic structure of the oxide halides. Both groups found that the electronic structures of these compounds are very similar to other high T_c cuprates, and most notably the replacement of the apical oxygen by the fluoride ion has little influence on the important electronic states close to the Fermi energy.

Examination of alternative synthetic strategies revealed that these new superconductors could also be obtained by simple solid-state reactions between $Sr_{2-x}A_xCuO_3$ and fluorinating agents such as NH_4F and MF_2, where M is a transition metal (e.g., CuF_2, ZnF_2, NiF_2, AgF_2 (12, 15). In this way, the toxicity and obvious handling problems associated with elemental F_2 gas can be easily avoided.

These studies have shown that fluorination can offer an important and powerful chemical route for the control of electronic and structural properties in materials and is comparable with the more commonly used methods of aliovalent cation substitutions and oxidizing/reducing annealings, e.g., in O_2 or N_2. We describe here a study of the fluorination of the mixed-metal cuprates $Sr_{2-x}A_xCuO_3$ and compare their behavior with that found for other Sr–Cu–O compounds. The differences in reactivity of the various

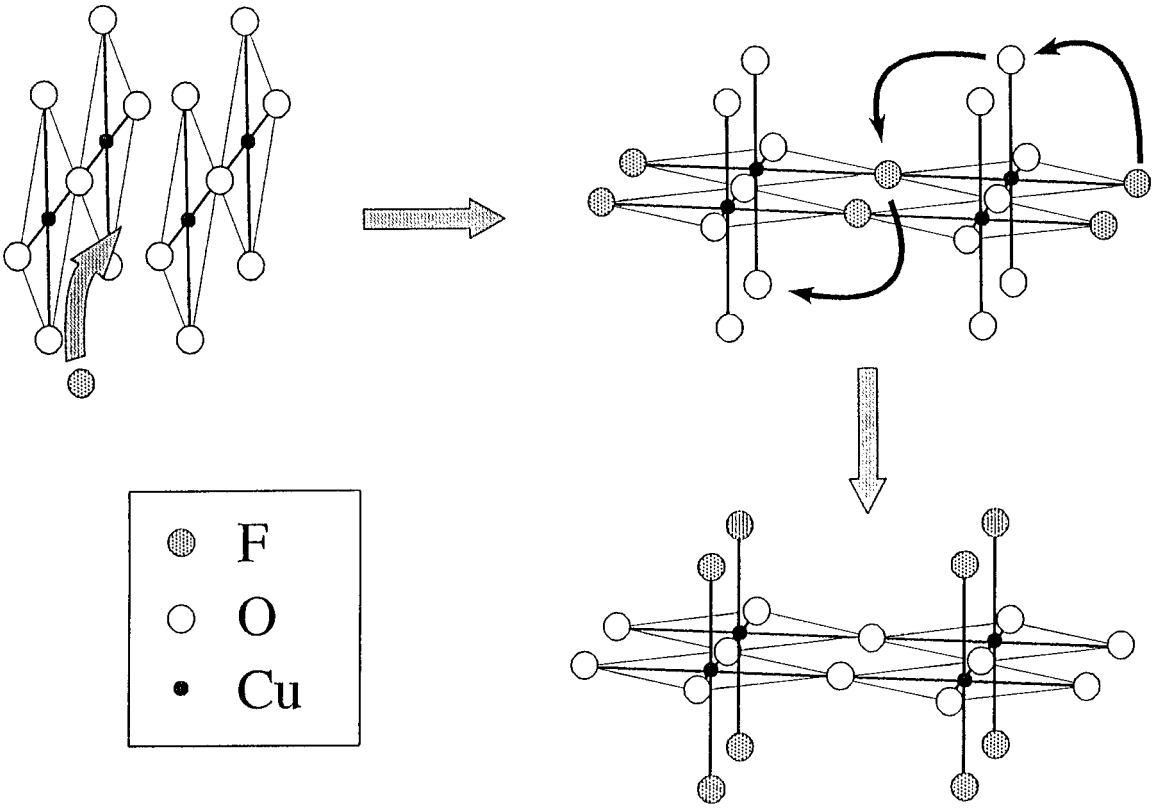

FIG. 2. Schematic representation of the structural rearrangement induced by fluorination in $Sr_{2-x}A_xCuO_3$ and leading to the formation of the CuO_2 planes in $Sr_2CuO_2F_{2+\delta}$.

cuprates toward fluorination are attributed to intrinsic structural differences in the parent alkaline earth cuprate. We present a comparison of the chemical mechanisms of the reactions involved in the different fluorination routes and an analysis of the nature of the structural rearrangements that occur during fluorination of the alkaline earth cuprates. A_2CuO_3 (A = Ca, Sr, Ba).

SUMMARY OF THE EXPERIMENTAL PROCEDURES

Direct Fluorination Using F_2—Method I

Starting materials were subjected to thermal treatments in a nickel furnace tube in a mixture of $10\%F_2/90\%N_2$ from which traces of HF had been removed by passing over NaF; Fig. 4 is a schematic representation of the fluorination apparatus. Typically, a 200-mg sample of starting material in a nickel boat was heated to 200–250 °C in dry N_2, subjected to a flowing F_2/N_2 atmosphere for 15 min at this temperature, and then allowed to cool in N_2 or air after flushing all F_2 from the system. In order to induce superconductivity in fluorinated $Sr_{2-x}A_xCuO_3$, samples were then typically annealed for up to 3 h in N_2 (temperatures up to 330°C, $0.4 \leq \delta \leq 0.6$) or for 15 min in a 10% H_2/N_2 mixture (temperatures up to 220°C, $0.2 \leq \delta \leq 0.4$).

Fluorination Using NH_4F—Method II

Ammonium fluoride (typically 4–6 moles of NH_4F per mole of $Sr_{2-x}A_xCuO_3$) was added to the $Sr_{2-x}A_xCuO_3$ samples and the mixture was ground, heated at 100 to 225°C/h, and then held at this temperature for 6–8 h under either an O_2 or air atmosphere. No further reduction was required to induce superconductivity in the $Sr_{2-x}A_xCuO_2F_{2+\delta}$ (A = Ba, Ca) samples.

Fluorination using MF_2 (M = Zn, Cu, Ag, Ni)—Method III

The anhydrous transition metal difluoride, 1.1–1.3 moles of MF_2 (M = Cu, Zn, Ag, Ni) per mole of $Sr_{2-x}A_xCuO_3$, was added to the precursor oxide $Sr_{2-x}A_xCuO_3$ and the mixture was ground and heated at 100 to 230°C/h and then held at this temperature for 6 h in air. For A = Ca, slightly higher temperatures were required to effect a complete reaction as the Ca content, x, was increased (e.g., 240°C for $x = 1$, 250°C for $x = 2$). No further reduction was required to induce superconductivty in the $Sr_{2-x}A_xCuO_2F_{2+\delta}$ (A = Ba) samples providing only 1.1–1.15 moles of MF_2 were added (1.3 moles led to an overdoped compound).

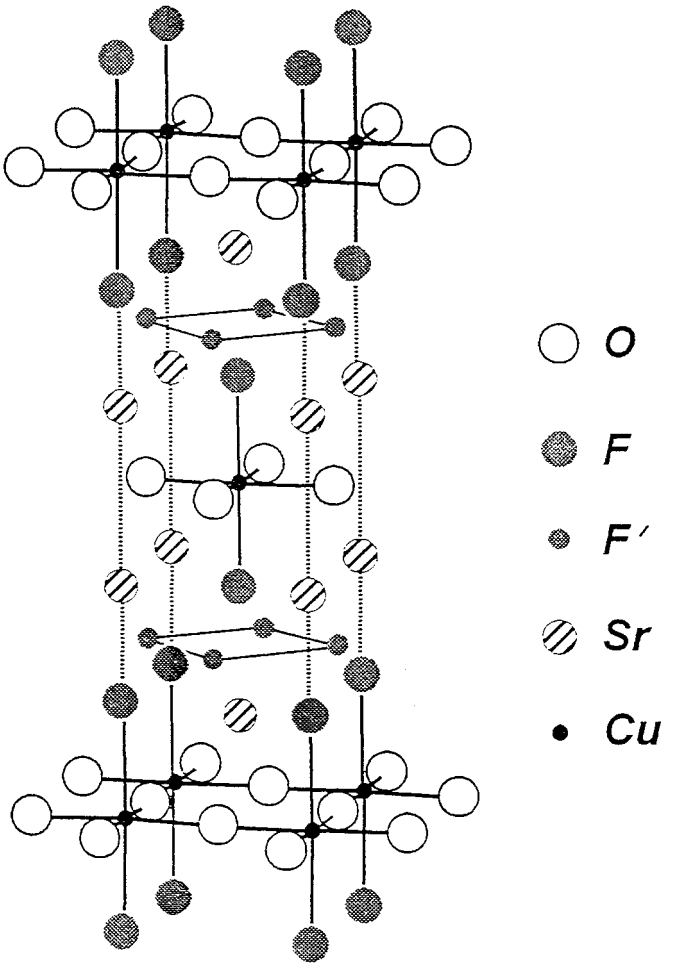

FIG. 3. Crystal structure of $Sr_2CuO_2F_{2+\delta}$; F is the substitutional fluorine, F′ is the interstitial fluoride ion.

RESULTS

Fluorination of $Sr_{2-x}A_xCuO_2F_{2+\delta}$ ($A = Ba, Ca$; $0.0 \leq x \leq 2.0$)

Methods I (F_2) and III (MF_2) were successful in forming all the $Sr_{2-x}A_xCuO_2F_{2+\delta}$ oxide fluorides ($A = Ca$, $0.0 \leq x \leq 2.0$; $A = Ba$, $x \leq 0.6$ and $x = 2$ for single-phase samples), whereas Method II m(NH_4F) was unsuccessful for high calcium levels ($x > 1.2$). Figure 5 shows X-ray powder diffraction (XRD) data from Sr_2CuO_3 and $Sr_2CuO_2F_{2-\delta}$ obtained by all three methods. The broad XRD peaks from the fluorinated materials are indicative of small crystallites. From the width of the X-ray peaks we estimated an average particle diameter of about 700 Å; similar crystallite sizes for the resulting oxide fluoride have also been indicated by electron microscopy (16, 17). Figure 5 indicates that the purest and best crystallized samples of $Sr_2CuO_2F_{2+\delta}$ are obtained from Methods I (F_2) and III (MF_2). The problems of the former route are the toxicity of F_2, the subsequent postsynthesis reduction treatments of the $Sr_2CuO_2F_{2+\delta}$ phase required to obtain the optimum T_c (5) and the limitation on the sample size that can be routinely prepared (ca. 200 mg). Interestingly, Method II (NH_4F) requires no postsynthesis reduction step to induce superconductivity in the samples, but unfortunately large quantities of (Sr, Ca, Ba)F_2 are produced as a by-product, (Fig. 5c). In addition, $Ca_2CuO_2F_{2+\delta}$ cannot be prepared satisfactorily by this route. The advantages of Method III (MF_2) are its simplicity and versatility; large samples of high purity can readily be prepared and fluorination of Ca_2CuO_3 can also be achieved by this method. The only problem is the presence of MO impurity (CuO in the case of CuF_2, Fig. 5d) in the final product due to the decomposition of MF_2. However, since the quantity of this impurity corresponds exactly to the amount of MF_2 added, due allowance can be made in subsequent chemical analyses.

Superconductivity was observed for $Sr_{2-x}Ba_xCuO_2F_{2+\delta}$ samples, with T_c generally increasing with increasing Ba content from 46 K ($x = 0$) to a maximum of 64 K for $Sr_{1.4}Ba_{0.6}CuO_2F_{2+\delta}$ (Fig. 6). This is the highest T_c observed for materials structurally related to La_2CuO_4. For Ca doping, the superconducting volume fraction progressively decreased from $\approx 4\%$ for $x = 0$ to zero (nonsuperconducting) for $x > 1$; for $0 < x < 1$, T_c remained at around 40–46 K. It should be noted that the Meissner fraction is always low (typically $< 10\%$) for superconducting oxide fluorides prepared using low-temperature routes, but this is to be expected for such samples, which consist of crystallites with dimensions comparable to the expected penetration length.

Structure refinements (using neutron powder diffraction data) of both $Sr_2CuO_2F_{2+\delta}$ and $Ca_2CuO_2F_{2+\delta}$ (5, 18) suggested that whereas the former is related to La_2CuO_4 (T structure, Fig. 3), the latter has the Nd_2CuO_4 structure (T', Fig. 7). Therefore, in spite of the fact that the parent phases Sr_2CuO_3 and Ca_2CuO_3 are isostructural, the resulting oxide fluorides $Sr_2CuO_2F_{2+\delta}$ and $Ca_2CuO_2F_{2+\delta}$ have fundamentally different structures. Ionic size tolerance factors have been estimated to probe the nature of this difference. The tolerance factor, t, for a perovskite lattice ABO_3, is defined by $t = (r_A + r_0)/\sqrt{2}(r_B + r_0)$, where r_A, r_B, and r_0 are the ionic radii of the large cation, small cation and anion, respectively. Average cationic and anionic radii (based on the ratios of O/F and Sr/A) were used to estimate the tolerance factors for the $Sr_{2-x}A_xCuO_2F_2$ system ($A = Ca, Ba$; $0 \leq x \leq 2$) and the results are listed in Table 1. Although the use of averaged radii provide only an approximate guide, the results suggest that the structures of $Sr_{2-x}A_xCuO_2F_{2+\delta}$ phases are linked to differences in anion/cation radius ratios. Tolerance factors have previously been used to rationalize the occurrence of the T and T' structures in mixed metal oxides of A_2BO_4 stoichiometry, especially the lanthanide oxides Ln_2CuO_4 (19). The T struc-

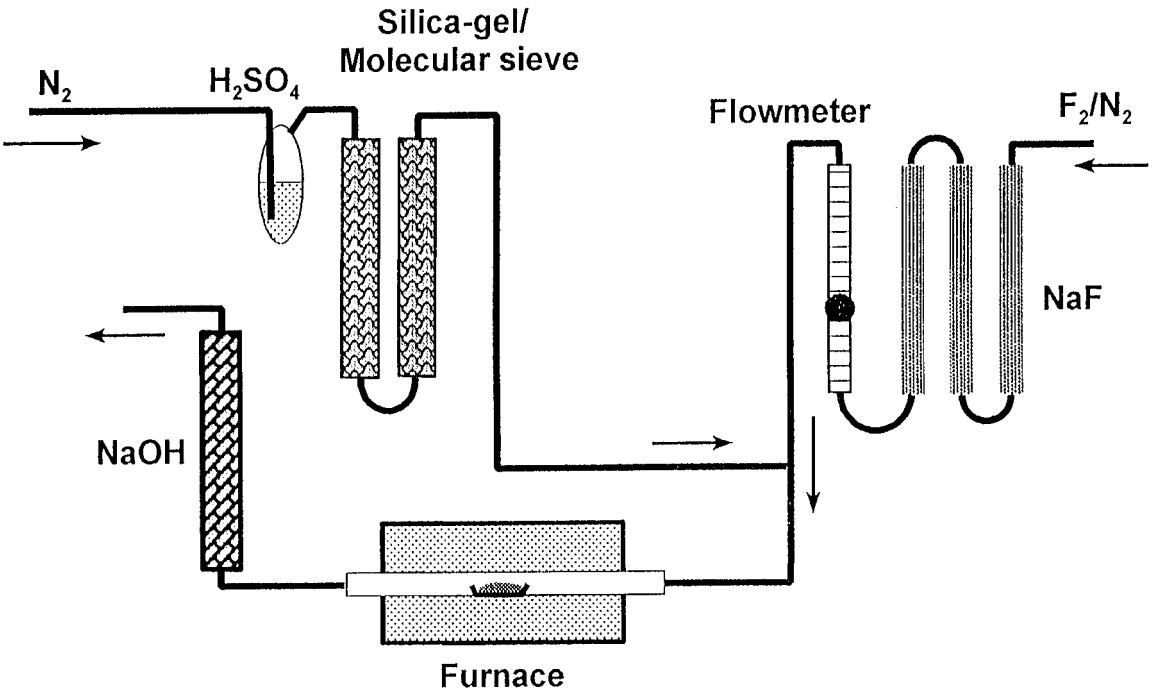

FIG. 4. Schematic diagram of gas-phase fluorination apparatus.

ture is related to the perovskite structure and contains layers of vertex-sharing octahedra separated by A ions. The closer the tolerance factor is to unity, which represents the perfect fitting of the cation in the A site, the more stable the T structure is expected to be. For Ln_2CuO_4, Bringley *et al.* (19) found that the stability limits are $0.87 \leq t \leq 0.99$ for the T structures and $0.83 \leq t \leq 0.86$ for the T' structure. Accordingly, our estimates show that in the (Sr, Ca, Ba)–Cu–O–F system the $Sr_{2-x}Ba_xCuO_2F_{2+\delta}$ compounds with $x \geq 0$ are characterized by the T structure and a T/T' structural transition occurs in the $Sr_{2-x}Ca_xCuO_2F_{2+\delta}$ compounds for $x \geq 1.5$. It should be noted, however, that these structural data relate to phases containing excess fluorine, whereas the tolerance factor parameter strictly corresponds to the stoichiometric $Sr_{2-x}A_xCuO_2F_2$ composition. The estimated tolerance factors are high in the $Sr_{2-x}Ba_xCuO_2F_{2+\delta}$ compounds but naturally decrease as x decreases, whereas for $Sr_{2-x}Ca_xCuO_2F_{2+\delta}$, the tolerance factors increase as x decreases. Thus, in the (Sr, Ca, Ba)–Cu–O–F system, the extremes of t are provided by $Ba_2CuO_2F_{2+\delta}$ and $Ca_2CuO_2F_{2+\delta}$. These estimates suggest that most of the $Sr_{2-x}A_xCuO_2F_{2+\delta}$ samples should be characterized by the T structure, but a transition to T' is predicted in the $Sr_{2-x}Ca_xCuO_2F_{2+\delta}$ series for high Ca contents, in accordance with neutron powder diffraction data on $Sr_2CuO_2F_{2+\delta}$ and $Ca_2CuO_2F_{2+\delta}$ (5, 18). This structural transition is induced by the reduction in the average radius of the cation A when Sr is substituted by Ca. Interestingly, an identical structural transition occurs in the Ln_2CuO_4 system as the radius of the lanthanide Ln is reduced from La to Nd.

Madelung energies, calculated for different distributions of oxygen and flourine atoms in $Sr_2CuO_2F_{2+\delta}$ and $Ca_2CuO_2F_{2+\delta}$ using refined structural parameters (5, 18) indicated a substantial preference of O^{2-} for equatorial rather than apical positions (e.g., 11,072 kJ mol^{-1} compared with 10,138 kJ mol^{-1} for $Sr_2CuO_2F_{2+\delta}$) and supported the view that fluorine insertion causes O/F interchange to give CuO_2 planes. Whereas in $Sr_2CuO_2F_{2+\delta}$ all apical positions are occupied by F^- ions, the T' structure of $Ca_2CuO_2F_{2+\delta}$ results in F^- ions filling the anion sites which are situated midway between the adjacent Ca layers. The location of fluorine therefore results in octahedral Cu^{2+} (4 planar O and two apical F) in $Sr_2CuO_2F_{2+\delta}$, with interstitial F^- ions situated between the SrF rocksalt layers. In $Ca_2CuO_2F_{2+\delta}$, on the other hand, the principal and interstitial F^- sites are reversed such that the interstitial site is now located in the apical position. In the absence of any interstitial fluorine, the Cu is therefore in square planar coordination to four oxygens.

The different location of fluorine in $Sr_2CuO_2F_{2+\delta}$ and $Ca_2CuO_2F_{2+\delta}$ has been confirmed by measurements of X-ray emission and photoelectron valence band spectra (20).

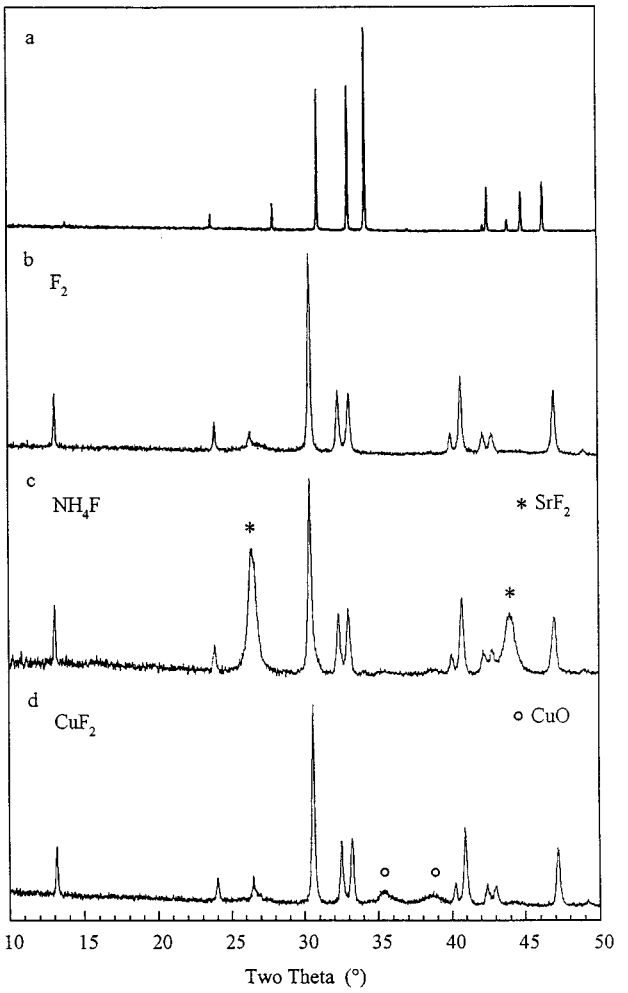

FIG. 5. X-ray powder diffraction patterns (Cu$K\alpha_1$) for (a) Sr_2CuO_3, and $Sr_2CuO_2F_{2+\delta}$ prepared by reaction of Sr_2CuO_3 with (b) F_2 gas, (c) NH_4F, and (d) CuF_2. Impurities are marked * (SrF_2) and ° (CuO).

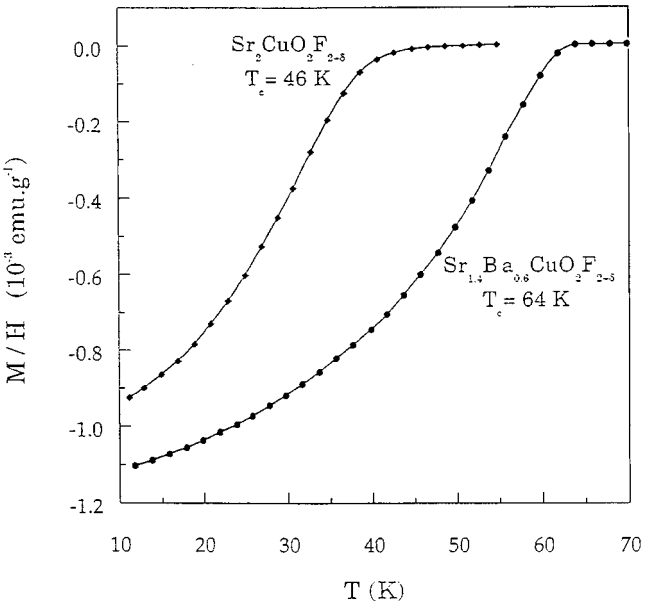

FIG. 6. Variation of the magnetic susceptibility of (a) $Sr_2CuO_2F_{2+\delta}$ and (b) $Sr_{1.4}Ba_{0.6}CuO_2F_{2+\delta}$ with temperature; relevant values of T_c are indicated.

Fluorination of Other Sr–Cu–O Systems

We have extended our investigations to other alkaline earth cuprates with structures containing chains of linked square CuO_4 units, viz $SrCuO_2$ (21) and $Sr_{14}Cu_{24}O_{39+\delta}$ (22). The XRD pattern of fluorinated $SrCuO_2$ shows small peak shifts to lower angles, consistent with a small expansion and a low level of fluorine incorporation. Minor structural changes were also inferred from a similar fluorination study of $Sr_{14}Cu_{24}O_{39+\delta}$; in this case, however, peak broadening accompanied small peak shifts, rendering reliable interpretation difficult. A degree of structural degradation appears to occur, associated with the insertion of a very small amount of flourine. Further work is planned to clarify the structural changes involved in fluorination of this material.

DISCUSSION

Fluorination Routes

The most important feature of all the fluorination methods discussed here is that the basic chemical reaction to form alkaline earth copper oxide fluorides must be carried out at relatively low temperatures (200–400°C) to impose a kinetic constraint on decomposition to the thermodynamically stable alkaline earth difluorides CaF_2, SrF_2, and BaF_2. In fact, conventional solid-state reactions involving oxides (or carbonates) and fluorides of the appropriate cations produce no oxide fluoride but a mixture of MO_n and AF_n, since $A_2MO_2F_{2+\delta}$ decomposes above ≈ 400°C.

The general scheme for direct fluorination, method I, is

$$Sr_{2-x}A_xCuO_3 + (1+\delta/2)F_2 \rightarrow Sr_{2-x}A_xCuO_2F_{2+\delta} + 1/2O_2.$$

The value of δ, which represents the fluorine located in the interstitial sites F′ in Figs. 3 and 7), and the purity of the resulting oxide fluoride are strongly dependent on both the temperature and the duration of the fluorination reaction. The optimization of these synthesis parameters led to the production of single-phase oxide fluorides, but never to optimally doped samples, such that subsequent annealing in N_2 was required to remove some of the excess fluorine.

Method II (NH_4F) appears a useful alternative since the superconducting transition temperature of the as-synthesized oxide fluorides indicates optimal doping. The metod is, however, not without its problems; in fact, the

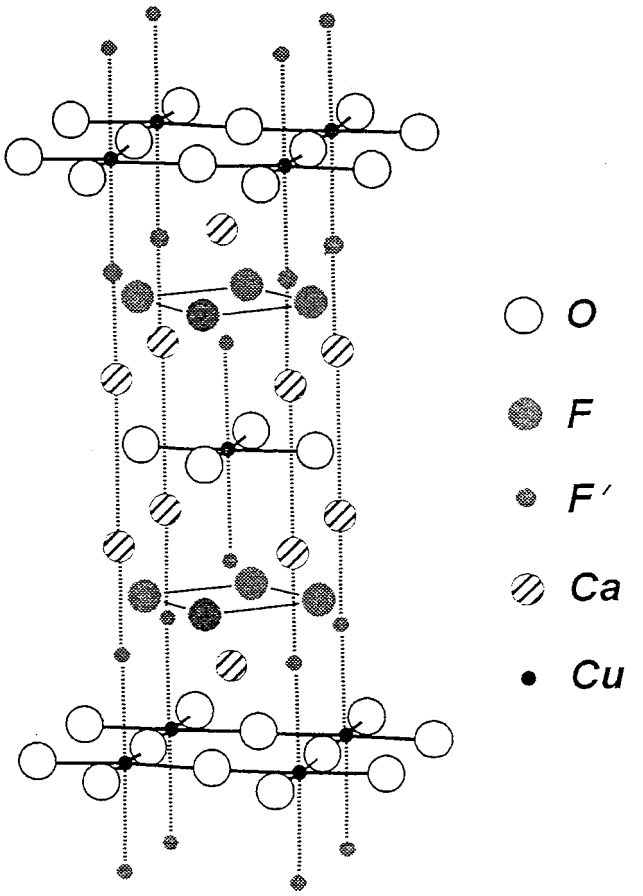

FIG. 7. Crystal structure of $Ca_2CuO_2F_{2+\delta}$; F and F′ are the substitutional and interstitial fluorine.

TABLE 1
Tolerance Factors (Estimated for the Ideal $Sr_{2-x}A_xCuO_2F_2$ Compositions) for Selected $Sr_{2-x}A_xCuO_2F_{2+\delta}$ (A = Ca, Ba) Compositions and Predicted Structure Types

Formula	Estimated tolerance factors	Predicted structure
$Ba_2CuO_2F_{2+\delta}$	0.957	T
$Ba_{1.5}Sr_{0.5}CuO_2F_{2+\delta}$	0.943	T
$SrBaCuO_2F_{2+\delta}$	0.930	T
$Sr_{1.5}Ba_{0.5}CuO_2F_{2+\delta}$	0.916	T
$Sr_2CuO_2F_{2+\delta}$	0.903	T
$Sr_{1.5}Ca_{0.5}CuO_2F_{2+\delta}$	0.892	T
$SrCaCuO_2F_{2+\delta}$	0.881	T
$Sr_{0.5}Ca_{1.5}CuO_2F_{2+\delta}$	0.870	T/T'
$Ca_2CuO_2F_{2+\delta}$	0.860	T'

oxide fluoride $Ca_2CuO_2F_{2+\delta}$ cannot be formed by the reaction Ca_2CuO_3 with NH_4F, although this phase can be readily prepared using F_2 gas. Moreover, large amounts of $(Sr/Ba)F_2$ impurities are produced and these alkaline earth fluoride impurities render rigorous chemical analysis of the superconducting phase very difficult. The stoichiometry of the superconducting oxide fluorides is therefore, to a large extent, dependent on structural analysis.

The formation of oxidized products (typical Cu oxidation state 2.3+) using Method II (NH_4F) presents us with an interesting mechanistic problem, since NH_4F is generally assumed to be nonoxidizing. It has been proposed (23) that decomposition of NH_4F may occur to provide elemental F_2

$$2NH_4F + 2O_2 = N_2 + F_2 + 4H_2O.$$

This process appears plausible since it produces not only elemental F_2, for subsequent oxidative fluorination, but also H_2O which would react with the moisture sensitive A_2CuO_3 oxide precursors. Fluorination of the decomposition products is then likely to result in the observed high levels of AF_2 impurities. However, the formation of F_2 from NH_4F and O_2 is thermodynamically unlikely given the rapid reaction of F_2 with H_2O to give HF. It seems likely, therefore, that direct reaction of NH_4F with the solid cuprate must occur to modify the thermodynamics; for example, adsorption of NH_4F on to the oxide might facilitate direct insertion of F atoms into the solid without the formation of F_2 molecules. Lattice energy effects may then provide the necessary thermodynamic driving force and the overall reaction might then be represented

$$(2+\delta)NH_4F + (3+2\delta)/2O_2 + A_2CuO_3 = A_2CuO_2F_{2+\delta} + (2+\delta)/2N_2 + 2(2+\delta)H_2O.$$

The formation of AF_2 impurities would still be explained by the production of H_2O. Such direct reaction with adsorbed NH_4F also allows rationalization of the different levels of fluorine incorporated by methods I and II as indicated by the superconducting properties of the "as prepared" samples. The thermodynamics of method II appear fundamentally different from those of method I, and any mechanisms invoking F_2 as an intermediate would be expected to yield products with similar fluorine contents. It is important to note that the oxidation of NH_4^+ (effectively NH_3) to N_2 in the above equation is not an essential feature and an alternative reaction in which NH_3 is evolved is probably more likely

$$(2+\delta)NH_4F + \delta/4O_2 + A_2CuO_3 = A_2CuO_2F_{2+\delta} + (2+\delta)/2H_2O + (2+\delta)NH_3.$$

In this process, HF and O_2 are respectively the fluorination and oxidation reagents. In order to demonstrate that HF is the vital component in this reaction mechanism, a direct

reaction between Sr_2CuO_3 and HF was performed by placing some Sr_2CuO_3 powder and 25 cm^3 of HF solution in an enclosed teflon bottle. The reaction was carried out in a microwave oven at $T \approx 120°C$ (the boiling point of the HF solution); the experiment resulted in the formation of $Sr_2CuO_2F_{2+\delta}$, albeit in small quantities, and a substantial amount of SrF_2, which presumably correlates with the high percentage of water in the HF solution. Moreover, experimental work on the reaction of cuprates with NH_4F performed on Ruddlesden–Popper cuprates, $Ln_{2-x}A_{1-x}Cu_2O_{6-y}$ (Ln = La, Nd; A = Ca, Sr), suggests that the reaction proceeds via the formation of HF (24). The fluorination reaction with NH_4F therefore appears to involve first the adsorption of NH_4F, followed by loss of NH_3, leaving HF incorporated in the sample. This then reacts to give a fluorinated sample and H_2O.

The use of method III (MF_2) for fluorination of $Sr_{2-x}A_xCuO_3$ (A = Ca, $0 \le x \le 2.0$; A = Ba, $0 \le x \le 0.6$) also eliminates the need for F_2 gas and, at the same time, produces negligible $(Sr/A)F_2$ impurity, unlike the corresponding fluorination with NH_4F, since H_2O and NH_3 are not generated in the reaction. In this respect, the use of MF_2 is preferable to NH_4F, since no cations appear to be extracted from the structure, and the potential problem relating to the precise cation stoichiomery of the product is reduced. Although MO (or M_2O for M = Ag) impurities (from the decomposed MF_2) are present in the samples, this does not constitute a serious problem for subsequent analysis of F content and Cu oxidation state because the quantity of the impurities can be calculated from the amount of the initial fluorinating agent. The results demonstrate that superconducting samples $Sr_{2-x}A_xCuO_2F_{2+\delta}$ (A = Ba, Ca) can be readily synthesized by fluorination of $Sr_{2-x}A_xCuO_3$ with trasition-metal difluorides, MF_2 (M = Cu, Zn, Ag, Ni), yielding similar T_c values (up to 64 K) as fluorination by F_2 gas or NH_4F (5, 12). This process appears to be a highly oxidative and versatile fluorination similar to F_2 gas, since overdoped samples of $Sr_{2-x}A_xCuO_2F_{2+\delta}$ can be obtained when excess MF_2 is used; the highly oxidative nature of the process has also been confirmed by the fluorination of other systems, e.g., fluorination of $Nd_{1.3}Sr_{1.7}Cu_2O_{6-x}$ using CuF_2 has been able to increase the Cu oxidation state from 2.0+ to 2.5+ (24). Moreover, the $Ca_2CuO_2F_{2+\delta}$ phase, which could not be prepared by the NH_4F route, is now readily synthesized.

A F/O exchange reaction between the starting alkaline earth oxide and the transition-metal fluoride such as

$$Sr_{2-x}A_xCuO_3 + MF_2 \rightarrow Sr_{2-x}A_xCuO_2F_2 + MO$$

is involved in this route. However, such a simple reaction cannot explain completely the formation of $Sr_{2-x}A_xCuO_2F_{2+\delta}$, since an exchange process of this type is not oxidative and, if the excess fluorine δ is taken into account, the amount of fluorine is unbalanced. Interestingly, the predicted products of such an exchange reaction, the stoichiometric phases $Sr_2CuO_2F_2$ and $Ca_2CuO_2F_2$, appear less stable than the fluorine-excess materials and cannot be synthesized using the methods described here. Fluorination of Sr_2CuO_3 with just one mole of MF_2, which might be expected to form stoichiometric $Sr_2CuO_2F_2$, instead gives superconducting $Sr_2CuO_2F_{2+\delta}$ ($\delta \approx 0.3$) and unreacted Sr_2CuO_3. Thus another process must take place concurrently with the exchange reaction. The similarities with method I (F_2) suggest that the reaction with transition-metal difluorides is associated with the generation of nascent F_2 gas. This is supported by the fact that in many cases fluorination can be successfully performed with the cuprate and MF_2 in separate boats in an enclosed autoclave (24). Elemental fluorine arises from the decomposition of the MF_2, due presumably to reaction with atmospheric O_2, i.e.,

$$MF_2 + 1/2O_2 \rightarrow MO + \text{“}F_2\text{”}.$$

The nascent F_2 so generated subsequently reacts with the cuprate. Assuming that the two processes are simultaneous, the general reaction scheme can be written

$$Sr_2CuO_3 + (1 + \delta/2)MF_2 + \delta/4\ O_2 \rightarrow Sr_2CuO_2F_{2+\delta} + (1 + \delta/2)MO.$$

The copper partial oxidation ($Cu^{II} \rightarrow Cu^{II}_{1-x} + Cu^{III}_x$) can also be taken into account within the reaction model

$$Sr_2CuO_3 + (1 + \delta/2)MF_2 + \delta/4\ O_2 \rightarrow Sr_2Cu^{II}_{1-\delta}Cu^{III}_{\delta}O_2F_{2+\delta} + (1 + \delta/2)MO.$$

This general scheme illustrates that the fluorine content, and hence the Cu oxidation state, is directly controlled by the quantity of MF_2 added. In this way, producing the optimum Cu oxidation state (2.2–2.3) should be straightforward. Experimental work is currently underway to determine whether the theoretical estimate of the amount of Cu(III) agrees with the experimental data.

Requirements for Superconductivity in the Sr/A–Cu–O–F Systems (A = Ca, Ba)

In order to correlate the structural characteristics of mixed-metal copper oxides with their behavior under fluorinating conditions, we have compared and contrasted several materials: $Sr_{2-x}A_xCuO_3$ (A = Ca, Sr), $Sr_{14}Cu_{24}O_{39+\delta}$ and $SrCuO_2$. All oxides in the Sr–Cu–O system which can be synthesized at 1 bar (25) were therefore included. These compounds differ structurally not only in the coordination geometry around Cu but also, and more importantly, in the method of linking of the Cu polyhedra. These different

TABLE 2
Structural Features for Selected Cuprates

Oxide	Copper Coordination and Linking	Schematic Representation
Sr_2CuO_3, Ca_2CuO_3	1-D chains from corner-linked CuO_4 squares	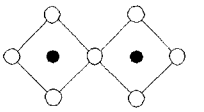
La_2CuO_4	Layers of corner-linked CuO_6 octahedra	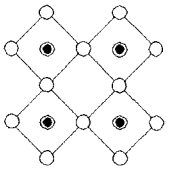
Nd_2CuO_4	Layers of corner-linked CuO_4 squares	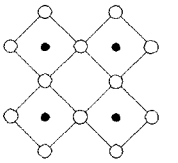
$SrCuO_2$	1-D double chains from edge-linked CuO_4 squares	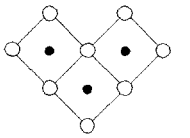
$Sr_{14}Cu_{24}O_{39+\delta}$	Corner- and edge-linked CuO_4 squares	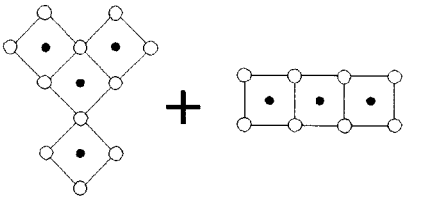

structural features have been summarized in Table 2, where, for comparison purposes, appropriate features for La_2CuO_4 and Nd_2CuO_4 have also been included.

Table 2 shows that these oxides differ in the way the copper polyhedra are linked within the structure: the polyhedra can be linked by corners, edges, or by a combination of corners and edges. Sr_2CuO_3, Ca_2CuO_3, La_2CuO_4, and Nd_2CuO_4 all contain exclusively corner-linked polyhedra. In the isostructural Sr_2CuO_3 and Ca_2CuO_3, this arrangement gives rise to 1-D infinite chains, whereas, in the latter two oxides, a 2-D infinite network of CuO_2 planes is observed. These 2-D CuO_2 planes are considered very important for the occurrence of superconductivity in suitably doped La_2CuO_4 and Nd_2CuO_4. We note that neither La_2CuO_4 nor Nd_2CuO_4 undergo significant structural rearrangement during fluorination: the extended 2-D CuO_2 network is already present in the structure and in $La_2CuO_4F_\delta$ the excess of fluorine is located in interstitial sites (26), whereas in $Nd_2CuO_{4-\delta}F_\delta$ simple F/O substitution is favored (27). $SrCuO_2$ contains extended parallel double chains of edge linked Cu–O square planar polyhedra, whereas $Sr_{14}Cu_{24}O_{39+\delta}$ is very complex and contains two interpenetrating structures of linked CuO_4 squares: one comprises 1-D chains of edge-linked polyhedra, while the other consists of 2-D sheets with mixed corner and edge shared polyhedra (22). The $SrCuO_2$ structure is closely related to that of Sr_2CuO_3, but contains a double Cu–O chain, with a short Cu–Cu distance of 2.8 Å (21). Similar chains are also present in $Sr_{14}Cu_{24}O_{39+\delta}$, but here they are corner-linked to form the 2-D extended sheets. As mentioned previously, these oxides differ from $(Sr, Ca, Ba)_2CuO_3$ in that fluorination does not induce large structural rearrangements. This is probably related to the fact that oxygen migration from the apical sites to the plane sites appears to be an important part of the mechanism of fluorination in the $(Sr, Ca, Ba)_2CuO_3$ oxides (Fig. 2). Oxygen

migration in perovskite-like oxides seems to take place along the octahedral edges (28), so that in structures containing edge-shared polyhedra, such migration may be hindered, In addition, if edge-shared CuO_4 units increase their coordination to form CuO_4F_2, edge-shared octahedra result, which are inherently less stable than corner-linked octahedra. This suggests that the isolated 1-D infinite chains of CuO_4 squares, which are present in A_2CuO_3, strongly favor fluorination and the consequent anion lattice rearrangement to give CuO_2 planes. This arrangement is quite rare, and, to the best of our knowledge, for cuprates is restricted to the $(Sr, Ca, Ba)_2CuO_3$ structure.

The fluorination reaction of these compounds results in both substitution and insertion of fluorine, which give rise to superconductivity in $Sr_2CuO_2F_{2+\delta}$ but not in $Ca_2CuO_2F_{2+\delta}$ (18). The lack of superconductivity in $Ca_2CuO_2F_{2+\delta}$ may be rationalized in three ways. One problem with $Ca_2CuO_2F_{2+\delta}$ is that insufficient interstitial fluorine can be incorporated to induce superconductivity, presumably due to the small size of the unit cell. For $Ca_2CuO_2F_{2+\delta}$, δ is typically 0.1 (18) giving a Cu oxidation state of 2.1, which is expected to be insufficient to induce superconductivity. To overcome this problem, Na/K doping could possibly increase the copper oxidation state, and supercoductivity in the oxide chloride $Ca_{2-x}Na_xCuO_2Cl_2$ has been achieved by such doping (29). However, it should be noted that these materials have different structures: $Ca_2CuO_2F_{2+\delta}$ has the T' structure, $Ca_{2-x}Na_xCuO_2Cl_2$ has the T structure. A second feature worthy of consideration is the fact that the T' structure is known to favor *n*-type rather *p*-type superconductivity (30). It has been proposed that the different superconducting behavior of La_2CuO_4 and Nd_2CuO_4 is related to the lattice mismatch bewteen the CuO_2 layers and the La–O/Nd–O blocks. In La_2CuO_4, the mismatch places the CuO_2 planes under compression favoring (oxidative) hole doping, whereas in Nd_2CuO_4, the CuO_2 planes are placed under tension, thus favoring (reductive) electron doping (31, 32). This feature is reflected in the equatorial Cu–O bond lengths (1.895 Å for La_2CuO_4, 1.975 Å for Nd_2CuO_4) and it is therefore interesting to compare Cu–O distances in relevant oxides and oxide fluorides, Table 3. It is pertinent to note that the Cu–O bond length in $Ca_2CuO_2F_{2+\delta}$ is relatively short (1.925 Å) and, in fact, is similar to that observed for $Sr_2CuO_2F_{2+\delta}$ (1.928 Å), which is a *p*-type superconductor. In addition, *p*-type superconductivity has also been observed in $Tm_{1.83}Ca_{0.17}CuO_4$ (Cu–O bond distance = 1.916 Å, T' structure) (33). Therefore, in principle, *p*-type superconductivity should be feasible in $Ca_2CuO_2F_{2+\delta}$, given appropriate electronic control. The final possible explanation relates to the location of the excess interstitial fluorine in the crystal structure. For $Ca_2CuO_2F_{2+\delta}$, these ions are located in the apical sites, i.e., close to the Cu ion (Cu–F = 2.41(2) Å (18)). Therefore, although the majority of copper ions will have square planar coordination, the small fluorine excess, δ, produces some with a square pyramidal configuration. These interstitial F^- ions are responsible for injecting the hole carriers in the CuO_2 sheets, but these holes must be delocalized to give rise to superconductivity. The presence of a mixture of square planar and square pyramidal Cu may be expected to create charge inhomogeneity on the CuO_2 plane, since the square pyramidal Cu^{2+} ions might act as centres for hole trapping. Therefore, to induce superconductivity we would require $\delta = 0$, and the doping of holes (*p*-type) or electrons (*n*-type) would require cation substitutions similar to those mentioned above. This intriguing possibility, noted also by Novikov *et al.* (11), brings our discussion full circle in that site-specific cation doping may prove to be a particularly fruitful line of future enquiry. In addition to being two alternative appoaches to electronic control of superconductivity in cuprate materials, cation and anion doping may also be employed in tandem to produce further exciting developents in this area of research.

TABLE 3
Equatorial Cu–O Distances in Cuprates and Copper–Oxide Fluorides

Samples	Cu–O distances (Å)
La_2CuO_4	1.895
Nd_2CuO_4	1.975
$Sr_2CuO_2F_{2+\delta}$	1.928
$Ca_2CuO_2F_{2+\delta}$	1.925
$Ba_2CuO_2F_{2+\delta}$*	1.965
$Sr_{1.4}Ba_{0.6}CuO_2F_{2+\delta}$*	1.934

For all samples, the Cu–O distances have been calculated from neutron diffraction data except for $Sr_{1.4}Ba_{0.6}CuO_2F_{2+\delta}$ and $Ba_2CuO_2F_{2+\delta}$ (*), where X-ray diffraction data were used.

CONCLUSIONS

The first superconducting oxide fluoride $Sr_2CuO_2F_{2+\delta}$, was prepared at low temperature ($200°C \leq T \leq 250°C$) either by reaction between Sr_2CuO_3 and F_2 gas or by solid-state reaction between Sr_2CuO_3 and a fluorinating agent (5, 12, 15). The synthesis of $Sr_2CuO_2F_{2+\delta}$ cannot be performed by conventional solid-state reaction at high temperature, but only by low-temperature fluorination of the parent compound Sr_2CuO_3; in fact $Sr_2CuO_2F_{2+\delta}$ is metastable and can be synthesized only by soft-chemistry fluorination pathways. These routes allow both fluorine substitution and insertion within the Sr_2CuO_3 structure, resulting in a significant structural reconstruction: 1-D Cu–O chains are converted into extended CuO_2 planes in $Sr_2CuO_2F_{2+\delta}$. These chemically induced changes also transform the semiconducting Sr_2CuO_3 into the high-temperature superconductor $Sr_2CuO_2F_{2+\delta}$.

We believe that these low-temperature fluorination methods can in principle be employed in other systems to change or deeply influence both physical and structural properties of other suitable compounds. Here we have attemped to highlight the important chemical reactions and the structural rearrangement involved to identify the relevant control parameters which most influence the synthesis and the properties of the resulting compounds.

The most convenient route for the flourination of compounds is the solid-state reaction between the precursor alkaline earth cuprate and a transition-metal fluoride as a fluorinating agent; by this route good quality and reproducible samples are obtained. It also seems possible to estimate approximately the average copper oxidation number in the resulting oxide fluoride by the amount of fluorinating agent used in the reaction.

A study of the structural rearrangement which takes place during the fluorination of the alkaline earth cuprates $Sr_{2-x}A_xCuO_3$ suggests that only oxides containing isolated 1-D infinite chains of corner-linked CuO_4 squares can undergo this particular type of major structural rearrangement which transforms Cu–O chains into extended CuO_2 planes in the structure.

ACKNOWLEDGMENTS

We thank the EPSRC for financial support. P.P.E. also thanks the Royal Society for the award of a Leverhulme Senior Research Fellowship.

REFERENCES

1. C. Greaves, M. Al-Mamouri, P. R. Slater, and P. P. Edwards, *Physica C* **235–240,** 158 (1994).
2. R. D. Shannon, *Acta Crystallaogr. A* **32,** 751 (1976).
3. P. Hagenmuller, *in* "Inorganic Solid Fluorides: Chemistry and Physics," p. 66. Academic Press, San Diego, 1985.
4. E. E. Fadeva, E. I. Ardashnikova, B. A. Popovkin, and M. P. Borzenkov, *Russ. J. Inorg. Chem.* **38**, 363 (1993).
5. M. Al-Mamouri, P. P. Edwards, C. Greaves, and M. Slaski, *Nature* (*London*) **369,** 382 (1994).
6. J. P. Hill, N. L. Allan, and W. C. Mackrodt, *Chem. Commun.* 2703 (1996).
7. M. S. Islam and S. Darco, *Chem. Commun.* 2291 (1996).
8. C. Chaillout, S-W. Cheong, Z. Fisk, M. S. Lehmann, M. Marezio, B. Morosin, and J. E. Schirber, *Physica C* **158,** 183 (1989).
9. P. G. Radaelli, J. D. Jorgensen, A. J. Schultz, B. A. Hunter, J. L. Wagner, F. C. Chou, and D. C. Johnston, *Phys. Rev. B* **48,** 499 (1993).
10. M. H. Tuilier, B. Chevalier, A. Tressaud, C. Brisson, J. L. Souberoux, and J. Etourneau, *Physica C* **200,** 113 (1992).
11. D. L. Novikov, A. J. Freeman, and J. D. Jorgensen, *Phys. Rev. B* **51,** 6675 (1995).
12. P. R. Slater, P. P. Edwards, C. Greaves, I. Gameson, J. P. Hodges, M. G. Francesconi, M. Al-Mamouri, and M. Slaski, *Physica C* **241,** 151 (1995).
13. T. Kawashima, Y. Matsui, and E. Takayama-Muromachi, *Physica C* **257,** 313 (1996).
14. E. Z. Kurmaev, V. R. Galakhov, V. V. Fedorenko, L. V. Elokhina, St. Bartkowski, M. Neumann, C. Greaves, P. P. Edwards, M. Al-Mamouri, and D. L. Novikov, *Phys. Rev. B* **52,** 2390 (1995).
15. P. R. Slater, J. P. Hodges, M. G. Francesconi, P. P. Edwards, C. Greaves, I. Gameson, and M. Slaski, *Physica C* **253,** 16 (1995).
16. E. I. Ardashnikova, S. V. Lubarsky, D. I. Denisenko, R. V. Shpanchenko, E. V. Antipov, and G. Van Tendeloo, *Physica C* **253,** 259 (1995).
17. B. Morosin, E. L. Venturini, J. E. Schirber, R. G. Dunn, and P. P. Newcomer, *Physica C* **241,** 181 (1995).
18. M. Al-Mamouri, P. P. Edwards, C. Greaves, P. R. Slater, and M. Slaski, *J. Mater. Chem.* **5,** 913 (1995).
19. J. F. Bringley, S. S. Trail, and B. A. Scott, *J. Solid State Chem.* **86,** 310 (1990).
20. E. Z. Kurmaev, L. V. Elokhina, V. V. Fedorenko, St. Bartkowski, M. Neumann, C. Greaves, P. P. Edwards, P. R. Slater, and M. G. Francesconi, *J. Phys. Condensed Matter* **8,** 4847 (1996).
21. M. T. Weller and D. R. Lines, *J. Solid State Chem.* **82,** 21 (1989).
22. E. M. McCarron III, M. A. Subramanian, J. C. Calabrese, and R. L. Harlow, *Mater. Res. Bull.* **23,** 1355 (1988).
23. X. Cheng, J. Liang, W. Tang, C. Wang, and G. Rao, *Phys. Rev. B.* **52,** 16233 (1995).
24. P. R. Slater, J. P. Hodges, M. G. Francesconi, P. P. Edwards, C. Greaves, and M. Slaski, in preparation.
25. N. M. Hwang, R. S. Roth, and C. J. Rawn, *J. Amer. Ceram. Soc.* **73,** 2531 (1990).
26. A. Tressaud, B. Chevalier, C. Robin, E. Hickey, and J. Etourneau, *Physica C* **185–189,** 583 (1991).
27. A. C. W. P. James, S. M. Zahurak, and D. W. Murphy, *Nature* (London) **338,** 240 (1989).
28. M. Cherry, M. S. Islam, and C. R. A. Catlow, *J. Solid State Chem.* **118,** 125 (1995).
29. Z. Hiroi, N. Kobayashi, and M. Takano, *Nature* (London) **371,** 139 (1994).
30. Y. Tokura, H. Tagagi, and S. Uchida, *Nature* (London) **337,** 345 (1989).
31. J. B. Goodenough, *Supercond. Sci. Technol.* **3,** 26 (1990).
32. K. Prassides and A. Lappas, *Chem. Br.* **30,** 730 (1994).
33. W. J. Zhu, Y. S. Yao, X. J. Zhou, B. Yin, C. Dong, Y. Z. Huang, and Z. X. Zhao, *Physica C* **230,** 385 (1994).